CORE
Metadata, citation and similar papers at core.ac.uk
Provided by Elsevier - Publisher Connector

Available online at www.sciencedirect.com
ScienceDirect
Biochimica et Biophysica Acta 1783 (2008) 98–106
Biochimica et Biophysica Acta
BBA
www.elsevier.com/locate/bbamcr

Embryonic stem cell differentiation studied by FT-IR spectroscopy

Diletta Ami [a,1,2], Tui Neri [b,2], Antonino Natalello [a], Paolo Mereghetti [c], Silvia Maria Doglia [a,*], Mario Zanoni [b], Maurizio Zuccotti [d], Silvia Garagna [b], Carlo Alberto Redi [b,e,*]

[a] *Dipartimento di Biotecnologie e Bioscienze, Università di Milano-Bicocca, Piazza della Scienza 2, 20126 Milano, Italy*
[b] *Laboratorio di Biologia dello Sviluppo, Dipartimento di Biologia Animale, Università degli Studi di Pavia, Piazza Botta 9, 27100 Pavia, Italy*
[c] *Dipartimento di Chimica, Università di Sassari, Via Vienna 2, 07100 Sassari, Italy*
[d] *Dipartimento di Medicina Sperimentale, Sezione di Istologia ed Embriologia, Università degli Studi di Parma, Via Volturno 39, 43100 Parma, Italy*
[e] *Fondazione IRCCS Policlinico San Matteo Pavia, Italy*

Received 11 May 2007; received in revised form 1 August 2007; accepted 2 August 2007
Available online 28 August 2007

Abstract

We propose, here, an FT-IR method to monitor the spontaneous differentiation of murine embryonic stem (ES) cells in their early development. Principal component analysis and subsequent linear discriminant analysis enabled us to segregate stem cell spectra into separate clusters – corresponding to different differentiation times – and to identify the most significant spectral changes during differentiation. Between days 4 to 7 of differentiation, these spectral changes in the protein amide I band (1700–1600 cm^{-1}) and in the nucleic acid absorption region (1050–850 cm^{-1}) indicated that mRNA translation was taking place and that specific proteins were produced, reflecting the appearance of a new phenotype. The DNA/RNA hybrid bands (954 cm^{-1} and 899 cm^{-1}) were also observed, suggesting that the transcriptional switch of the genome started at this stage of differentiation. As confirmed by cytochemical assays, the FT-IR approach presented here allows to detect at molecular level the biological events of ES cell differentiation as they take place and to monitor in a rapid way the temporal evolution of the ES cell culture.
© 2007 Elsevier B.V. All rights reserved.

Keywords: Cardiomyocyte; Cytodifferentiation; Embryonic stem cell; Fourier transform infrared spectroscopy; Linear discriminant analysis; Principal component analysis

1. Introduction

Embryonic stem (ES) cells are a unique self-renewing cell type that in culture can give rise to the ectodermal, endodermal, and mesodermal germ layers, mimicking embryogenesis [1–3].

ES cells can potentially generate every cell type in the body, making them excellent candidates for cell- and tissue-replacement therapies, with great potential for pharmaceutical screening and transplantation in a wide range of therapies [4]. ES cells arise from the inner cell mass of the mammalian blastocyst and can be propagated in culture in an undifferentiated state. When properly stimulated, they can be induced to differentiate selectively into more specialized populations. For instance, this can be achieved *in vitro* by transferring the cells to non-adherent plates in which they spontaneously form differentiated structures called embryoid bodies (EBs) [5] (for a review, see [6]).

The understanding of the developmental pathways by which ES cells differentiate into different tissue types is essential to exploit their therapeutic potential. To this end, it will be useful to develop new technological tools to study ES cell differentiation in a non-time-consuming way. Indeed, to monitor the differentiation status of cultured ES cells lengthy procedures are at present required, indicating the need for rapid and simple assays.

In this perspective, Fourier transform infrared (FT-IR) spectroscopy has been proven to be a powerful tool to detect changes in the macromolecular content of whole cells, through the absorption of electromagnetic radiation in the middle infrared range (from 4000 to 400 cm^{-1} wavenumbers) [7–12].

* Corresponding authors. S.M. Doglia is to be contacted at tel.: +39 02 6448 3459; fax: +39 02 64483565. C.A. Redi, tel.: +39 0382 986323; fax: +39 0382 98627.
E-mail addresses: silviamaria.doglia@unimib.it (S.M. Doglia), carloalberto.redi@unipv.it (C.A. Redi).
[1] Present address: Consortium for Genomic Technologies (COGENTECH), Biochemistry Unit, Via Adamello 16, 20139 Milano, Italy.
[2] These authors contributed equally to the work.

0167-4889/$ - see front matter © 2007 Elsevier B.V. All rights reserved.
doi:10.1016/j.bbamcr.2007.08.003

In particular, by the new developments of multivariate analysis [13] that allows a more efficient analysis of complex spectra, important information in cell biology and medicine was obtained [14–16]. Recently, these approaches have been successfully applied to the study of stem cell differentiation by a number of research groups [17–19]. Interestingly, FT-IR spectroscopy can contribute also to the characterization of substrates for stem cell growth and labelling [20–22].

Here, we describe the use of FT-IR microspectroscopy coupled with multivariate analysis to examine the infrared absorption of murine ES cells in order to identify their developmental status *in situ* through possible changes in their macromolecular content during differentiation. This approach is rapid, non-destructive and it allows examining the expression of different biomarkers simultaneously in a single absorption measurement.

Among other non-invasive spectroscopic techniques, Raman microspectroscopy has been recently applied to the *in situ* study of ES cells [23,24]. These authors were able to obtain important insights on ES cell differentiation through the response of the nucleic acid Raman bands. The infrared microspectroscopy study that we report here is in excellent agreement with the ES cell Raman investigation, a significant result since these two techniques are actually probing the vibrational properties of ES cells by a different interaction with the electromagnetic radiation.

In addition, it should be noted that infrared spectroscopy in the amide I region (1700–1600 cm^{-1}) is highly sensitive to protein secondary structure that can be determined for proteins in solution [25,26], within intact cells [27–29], tissues, and whole organisms [30,31]. In this work, we exploited this potential of infrared spectroscopy to evaluate not only the total protein content of ES cells but also the secondary structure of the proteins expressed during differentiation.

By FT-IR microspectroscopy we showed that, using a limited amount of intact cells (about 10^4 cells), it is possible to monitor the time course of ES cell differentiation as it takes place. Through the multivariate analysis of the ES differentiating cell spectra, we were able to identify the most significant spectral changes that occur in the protein and nucleic acid absorption regions. The support of biological assays enabled us to assign the observed changes in band position and intensity to specific molecular events taking place during ES cytodifferentiation.

2. Materials and methods

2.1. ES cell culture

Undifferentiated murine ES cells were cultured on a mitomycin-C (Sigma-Aldrich, Italy) inactivated STO feeder layer (a gift from Dr. Marina Morigi, Istituto di Ricerche Farmacologiche Mario Negri, Bergamo) (step 1), then passaged to gelatin-coated T75 flasks (step 2), both passages in Knockout DMEM supplemented with 20% ESC qualified fetal bovine serum, 2 mM L-glutamine, 1× non-essential amino acid solution, 0.5% penicillin–streptomycin solution (Invitrogen), 0.1 mM beta-mercaptoethanol (Sigma) and 500 U/ml of leukemia inhibitory factor (ESGRO-LIF, Chemicon International). Steps 1 and 2 were repeated to maintain ES cells undifferentiated. ES cells were passaged enzymatically every 2 days using 1× trypsin–EDTA solution (Invitrogen) and maintained in incubator at 37 °C and 7.5% CO_2 in air. Prior to FT-IR spectroscopy analyses, undifferentiated ES cells were cultured for 3 passages on T75 gelatin-coated flasks in a complete medium, to avoid STO contamination.

2.2. ES cell differentiation

After three passages on gelatin-coated flasks, colonies were dissociated to a single cell suspension and plated on new T75 gelatin-coated flasks in a LIF-free ES medium that was changed every 2 days to induce spontaneous differentiation. Following plating, differentiated ES cells were collected and prepared for FT-IR analysis at days 4, 7, 9 and 14. A total of three independent experiments were carried out.

2.3. Embryoid body formation

Embryoid bodies (EBs) were formed from about 2×10^3 ES cells using the hanging drop method (for a detailed explanation see [32–34]). EBs were collected at days 2, 4 and 7 days of differentiation.

2.4. Cytochemical analysis

In order to visualize areas of cardiomyogenic differentiation, as cardiomyocytes are rich in glycogen [35], PAS (periodic acid—Schiff) reaction was performed on cells at 0, 7 and 14 days of culture in two different experiments. Briefly, cells were rinsed in PBS and fixed with formyl alcohol (9:1 mixture of 95% ethanol and formaldehyde) for 15 min; fixative was removed, cells were rinsed with 95% ethanol, air-dried, rinsed twice with tap water, incubated for 10 min with 1% periodic acid, rinsed twice with tap water, stained with Schiff's reagent for 10 min, rinsed three times with sodium metabisulfite solution for 2 min and rinsed twice with tap water. All steps were carried out at room temperature. Areas of cardiogenic differentiation are visualized by intense purple colour staining. Alkaline phosphatase (AP) activity (Sigma Kit 85L-2) was detected in two different experiments on undifferentiated ES cells (time 0) and on 7 and 14 days spontaneously differentiated cells.

2.5. FT-IR microspectroscopy of ES cells

FT-IR microspectroscopy was performed on (a) undifferentiated ES cells, passaged three times on gelatin-coated T75 flasks and analyzed the day after the third passage, to benefit from maximum transcriptional activity; (b) differentiated ES cells at 4, 7, 9 and 14 days of culture in absence of LIF; (c) EBs at 2, 4, and 7 days of differentiation.

Before measurements, cells were always mechanically dissociated and washed three times in a physiological solution (0.9% NaCl in distilled H_2O) to eliminate medium contamination. 3 μl of the cell suspension were then deposited onto a BaF_2 window, and dried at room temperature for about 30 min to eliminate the excess of water.

Absorption spectra in the range from 4000 to 600 cm^{-1} were acquired in the transmission mode using a UMA 500 infrared microscope, equipped with a nitrogen cooled MCT detector (narrow band, 250 μm) and coupled to a FTS 40A spectrometer (both from Bio-Rad Laboratories, Digilab Division, USA).

Excellent spectra with high signal-to-noise ratio (peak-to-peak noise of 0.5 mA at 2000 cm^{-1}) were collected through a microscope diaphragm aperture of 100 μm × 100 μm, working at 20-kHz scan speed, 2 cm^{-1} spectral resolution, 128 scan co-additions and triangular apodization [36]. Spectra were corrected – when necessary – for the residual water vapour absorption by subtraction of the vapour spectrum.

A second derivative analysis of the spectra was performed – after a 13-point smoothing of the measured spectra – by the Savitzky–Golay method (3rd polynomial, 13 smoothing points), using the GRAMS/32 software (Galactic Industries Corporation, USA).

For each cell pellet deposited onto a BaF_2 window, several measurements were repeated by selecting different areas of 100 μm × 100 μm on the same cell sample through the variable diaphragm aperture of the infrared microscope. Within the same differentiation experiment, an excellent reproducibility of the spectra (in band intensities and positions) was obtained among measurements on the same cell pellet and on cell pellets taken from the same ES cell culture at each differentiation time—at 0, 4, 7, 9 and 14 days.

Table 1
Principal FT-IR bands of ES cells during spontaneous differentiation

Peak position from second derivative spectra (cm^{-1})	Wavenumbers from PCA-LDA		Assignment
	cm^{-1}	Loading	
1692.2±2.6	1693.7	0.15	β-Sheet protein secondary structure [25,26]
1682.5±1.0	1685.9	0.41	β-Turn protein secondary structure [25,26]
1656.7±1.3	1658.0*	0.80	α-Helix protein secondary structure [25,26]
	1656.1*	1.00	
	1653.2	0.62	
1638.7±1.3	1636.8	0.34	Intramolecular β-sheet [25,26]
	1632.9	0.38	
1030.0±2.5	1029.1	0.35	Glycogen [14,19]
1023.5±2.0	1023.4	0.41	
	1021.4	0.48	
994.2±2.2	994.4	0.21	Ribose phosphate main chain, ν and δ ring of uracil [8,43,44]
969.2±1.6	975.1	0.67	RNA ribose phosphate main chain [8,43,44]
966.0±0.6	962.6*	0.80	νCC of DNA backbone [8,43,44]
954.5±1.0	958.7*	1.00	νCC of DNA backbone [44]
	954.9*	0.90	
914.5±1.5	916.3	0.30	Ribose ring [44]
898.9±1.0	899.9	0.39	Deoxyribose ring [44]
	895.1	0.62	
888.0±2.0	889.3	0.64	DNA band [8]

Peak positions taken from second derivative of the measured absorption spectra, wavenumbers with higher loadings from PCA-LDA of second derivative spectra, and band assignment are reported.
* Wavenumbers with the highest contribution to the inter-spectral variance.

Three independent differentiation experiments were carried out. When comparing the spectra from independent experiments, band positions were highly reproducible within the spectral resolution of the measurements (see standard deviations reported in Table 1) whereas band intensities – taken from the area of the negative bands in the derivative spectra – displayed a standard deviation up to 20%. This result was actually expected if one considers the biological variance of the molecular content of ES cells that in different experiments can be affected by minor differences in the growing conditions.

On the contrary, the temporal occurrence of the band intensity changes during the time course of differentiation was highly reproducible from one experiment to another, indicating that the timing of molecular events during differentiation is strictly controlled.

2.6. Multivariate analysis

Raw spectra, first and second derivatives were processed using the principal component discriminant analysis (PCA-LDA) method [13,14]. All statistical analysis was performed using MatLab R2006a (The Mathworks, USA).

At first, PCA scores were obtained projecting the original data on the subspace defined by the selected eigenvectors of the covariance matrix. PCA scores were then used as input for LDA in which the class variable corresponded to the differentiation days. The selection of the number of eigenvectors considered in the PCA was carried out iteratively by repeating the PCA-LDA analysis: the number of eigenvectors was increased starting from 2 until the associated variance reached the value of 100% (25 eigenvectors for the row data, 23 for the first derivative, 22 for the second derivatives) choosing the lowest number of eigenvectors that led to the highest classification accuracy. The classification accuracy was computed as the fraction of correctly classified cases out of the total number of sample cases. In particular, to obtain a robust estimation of the accuracy the leave-one-out cross validation was performed.

The selection of the most relevant wavenumbers was performed considering the weighted sum of the PCA-LDA loadings defined as $\overline{wl} = \sum_{i=1}^{N} L\ \mathrm{diag}(C)$, where N is the total number of discriminant functions, L is the PCA-LDA loading matrix and C is the total covariance matrix [37]. The obtained averaged loading is then rescaled in the range 0–1.

Clusters, corresponding to the differentiation days, can be viewed on the 2D and 3D PCA-LDA score plots. To better visualize the separation among clusters, ellipses (2D plot) and ellipsoids (3D plot) were drawn centred on clusters mean. The semi-axes of the ellipses correspond to two standard deviations of the cluster data.

3. Results

3.1. ES cell differentiation and morphology

The ES cell line (UPV04) used in this study was produced in our laboratory following standard protocols [38] and it fulfilled criteria of pluripotency, as demonstrated by the presence within EBs of the derivatives of the three germ layers, i.e., ectoderm, mesoderm and endoderm [39] that were regularly tested during ES cell culture (data not shown).

Undifferentiated ES cells were grown in tight colonies with smooth shiny edges (Fig. 1A); when plated in a medium without LIF, they started to differentiate. Undifferentiated ES cell colonies were negative to PAS reaction, although a negligible number of colonies presented very small foci of PAS-positive reaction (Fig. 1B, arrows), indicating a spontaneous differentiation towards the mesoderm lineage (cardiomyogenic differentiation) [40].

Two days after LIF removal, colonies tended to flatten and form string-like structures. AP activity, appreciably high in undifferentiated ES cells (Fig. 1C), decreased during differentiation. One week after plating, two cell populations were present: cells residing in the core of the colonies with a small and round morphology (Fig. 1D) were negative to AP activity (Fig. 1F, arrowhead) but positive to the PAS reaction (Fig. 1E, arrows); cells residing at the edges of the colonies (Fig. 1D) remained positive to AP activity (Fig. 1F, arrow).

Two weeks after plating, few flat colonies were present together with many cells of various shapes, dispersed among the colonies and representing the derivatives of the three germ layers (Fig. 1G). The core of the colonies was negative to AP (Fig. 1I, arrowhead) and highly positive to PAS reaction (Fig. 1H, arrows) indicating areas of cardiomyogenic differentiation [35]; cells dispersed among the colonies – likely migrating from the edges of the colonies – were negative to PAS reaction (Fig. 1H, arrowhead) and still positive to AP activity (Fig. 1I, arrow).

3.2. Infrared absorption spectrum of ES cells

The FT-IR absorption spectrum of undifferentiated ES cells is reported in Fig. 2A. To better resolve the FT-IR spectrum, it was useful to perform the second derivative analysis of the spectrum (Fig. 2B). This is a mathematical procedure that allows to resolve broad bands made by the overlapping of

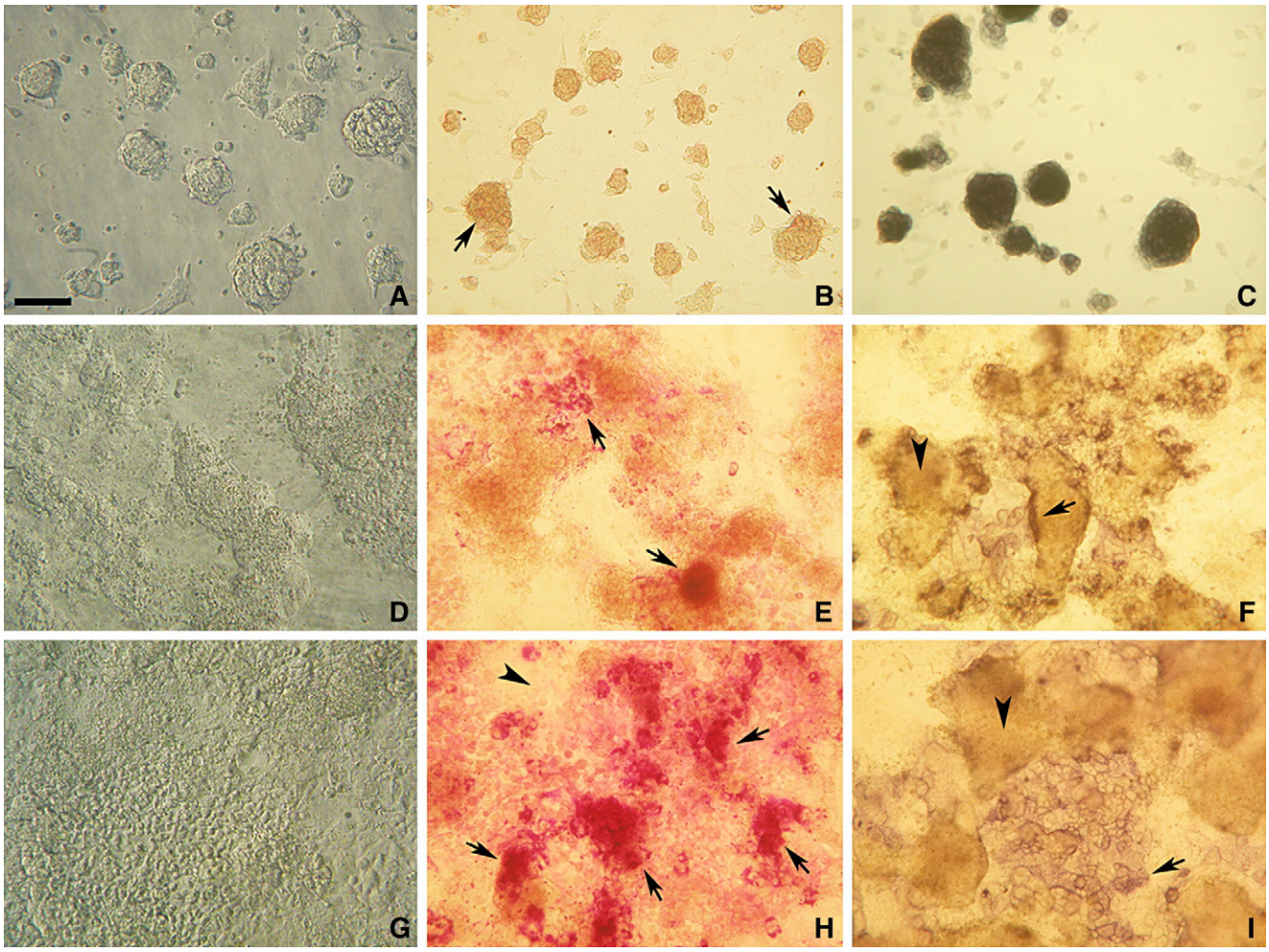

Fig. 1. ES differentiation into cardiomyocyte precursors. Undifferentiated cells: phase contrast microscopy image (A); small and weak purple PAS stained areas are distinguishable in few colonies (B, arrows); colonies have strong AP activity (C). ES cells 7 days from plating: phase contrast microscopy image (D); PAS stained areas of cardiomyogenesis are visible (E, arrows); AP activity is absent in the core of the colonies (F, arrowhead), but present at the edges of the colonies (F, arrow). ES cells 14 days from plating: phase contrast microscopy image (G); PAS reaction strongly stains cluster of cells in the core of the colonies, indicating large areas of cardiomyogenesis (H, arrows) while cells dispersed among the colonies are PAS negative (H, arrowhead); AP activity is restricted to the cells dispersed among the colonies (I, arrow), but it is not present in the core of the colonies (I, arrowhead). Scale bar: 100 μm.

several components, whose peak positions cannot be easily appreciated by visual inspection of the spectrum [25,26,41].

As can be seen, the spectrum of undifferentiated ES cells is highly complex, as is that of any other eukaryotic cell [8]. However, an efficient and reliable analysis of complex spectra can be performed by the use of multivariate analysis, as recently reported in the literature [13–19]. Principal component analysis and subsequent linear discriminant analysis [13,14] enabled us to segregate stem cell spectra into separate clusters (corresponding to different differentiation times) and to identify the most significant spectral changes during differentiation (Table 1). Most of them occurred in the protein amide bands (1700–1500 cm^{-1}), and in the nucleic acid region (1150–850 cm^{-1}) where the absorption of phosphate and ribose/deoxyribose moieties, as well as that of glycogen, can be found. In the following paragraphs we report the second derivatives of the measured ES spectra in the two selected regions, where important changes occur, as indicated by PCA-LDA analysis (Table 1, see separate paragraph).

3.3. Protein expression in ES cells during spontaneous differentiation detected through the amide I band analysis

The amide I band in the region from 1700 to 1600 cm^{-1} of the undifferentiated ES cells (Fig. 2A) gives information on the total cell protein content. As indicated by the second derivative analysis of the spectra (Figs. 2B and 3A), the secondary structure of the proteins expressed by the undifferentiated cells consisted mainly of three components (Fig. 3A and Table 1), that can be assigned to antiparallel β-sheets (1692 cm^{-1}), α-helices (1657 cm^{-1}) and intramolecular β-sheets (1639 cm^{-1}) [25,26]. As shown in Fig. 3A, the relative intensity of these components was seen to change when differentiation took place, indicating – as expected – that different proteins were expressed by the cells during differentiation.

The α-helix band intensity markedly increased after 4 days of differentiation. At this time, a minor component around 1682 cm^{-1} (see Table 1) was also observed and assigned to β-turn structures [25]. After 7 days of ES cell differentiation, the

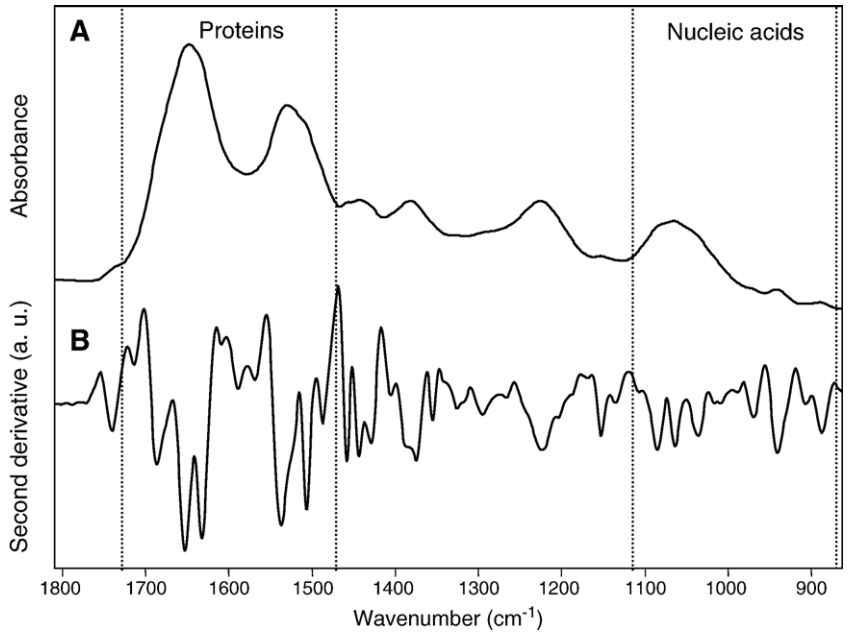

Fig. 2. FT-IR absorption spectrum of undifferentiated ES cells. FT-IR absorption spectrum of undifferentiated ES cells (A), and its second derivative (B).

increase of these two bands was more evident, while the β-sheet component at 1639 cm^{-1} remained approximately constant. This result clearly indicated that, from days 4 to 7, ES cells were expressing proteins with high α-helix and appreciable β-turn structures that can be the specific proteins of the new phenotype. Interestingly, during the first week of spontaneous differentiation, the presence of a population of cardiomyocyte precursors – rich in glycogen – was found by the positive PAS reaction (Fig. 1E and H) [35,40]. Actually, these cells are known to express high level of alpha-myosin, a protein belonging to the α-helix fold. In addition, gap junctions increase during ES cell differentiation, suggesting that also connexins – α-helix

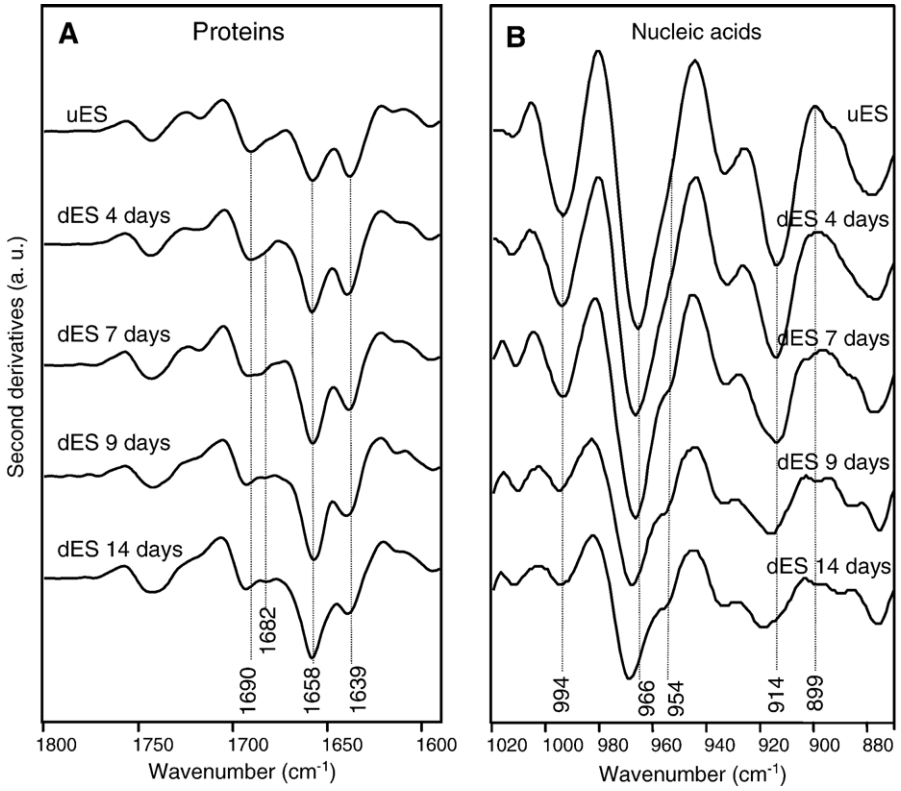

Fig. 3. FT-IR monitoring of ES cell spontaneous differentiation. Second derivatives of absorption spectra at different stages of ES differentiation (up to 14 days) in the protein amide I (A) and nucleic acid (B) absorption regions.

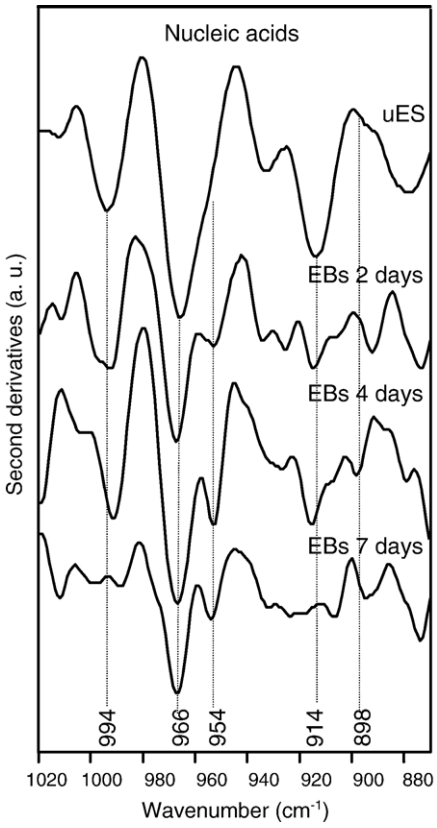

Fig. 4. FT-IR monitoring of ES cell differentiation via formation of embryoid bodies (EBs). Second derivatives of absorption spectra at different stages of ES cell differentiation (up to 14 days) in the nucleic acid absorption regions.

proteins containing an important percentage of β-turns – might be overexpressed [42]. Therefore, the sharp increase in the α-helix content from day 0 to day 10 of cell culture – and the presence of the β-turn secondary structure, undetectable in undifferentiated cells – could be taken as evidence of the appearance of cardiomyocyte precursors.

3.4. Spontaneous differentiation of ES cells monitored by nucleic acid infrared bands in the 1050–850 cm^{-1} region

In the absorption spectrum of undifferentiated ES cells three principal bands were identified and assigned ([8,43,44] and references therein) in the nucleic acid region from 1050 to 850 cm^{-1}. As can be seen in Fig. 3B and in Table 1, these bands respectively occurred at 994 cm^{-1} (ribose phosphate main chain mode), 966 cm^{-1} (DNA CC stretching of the backbone and RNA ribose phosphate main chain modes), and at 914 cm^{-1} (ribose ring mode). These bands, which are the spectral signatures of the RNA and DNA content of undifferentiated cells, were found to change in intensity and peak position during ES cell differentiation. The 994 cm^{-1} and 914 cm^{-1} RNA bands, both assigned to ribose vibrations, decreased up to day 9 of differentiation, as shown in Fig. 3B.

As differentiation started, an important decrease of the 966 cm^{-1} band intensity was also observed, indicating that the DNA content of undifferentiated cells decreased at the beginning of the differentiation process. After 4–7 days of ES cell differentiation, a minor but significant shoulder of the 966 cm^{-1} band became apparent around 954 cm^{-1} (CC stretching of DNA backbone). The presence of this new component and the simultaneous appearance of the deoxyribose ring vibration at 899 cm^{-1}, which can be assigned to a vibrational mode of A-DNA [44], indicate that also a DNA/RNA hybrid started to be present.

Furthermore, at day 7 of ES cell differentiation, a minor but significant shift was observed for the 966 cm^{-1} peak towards 969 cm^{-1}, due to the emergence of a new band that might be assigned to RNA [8,43,44].

These spectral features indicate that, when active transcription of the genome takes place in differentiating ES cells, proteins of the new phenotype are expressed, in accordance with what shown by the amide I analysis.

In addition, we should report that in this spectral region also the absorbance of glycogen occurs. In particular we observed the increase of the glycogen bands around 1023–1030 cm^{-1} starting at 7 days of differentiation, in agreement with the emergence of cardiomyocyte precursors – rich in glycogen – detected by the PAS reaction.

Interestingly, the spectral changes reported above in the nucleic acid region were also found for ES cell differentiation via embryoid body formation, where the behaviour of the 954 cm^{-1} and 899 cm^{-1} bands was even more evident, as shown in Fig. 4.

3.5. Multivariate analysis

The use of multivariate analysis, in particular principal component and linear discriminant analyses, enabled us to explore in an efficient way the spectra in the wide spectral range (1800–800 cm^{-1}) and to identify the significant spectral variations during differentiation.

This is made possible by the reduction of the original variables – the absorbance values of the spectra at the different wavenumbers – into a few principal components that can describe most of the spectral variance.

In PCA each spectrum is represented by a single point in the *n*-dimensional space, whose coordinates are the scores on the most significant principal components, which can be taken as axes for the score plot. Following the procedure reported by Fearn and Walsh et al. [13,14], we combined PCA with a linear discriminant analysis (LDA) to further process the PCA output. In LDA, new variables, which are the best linear combination of the original principal components to maximize the ratio between-group variance and within-group variance, lead to a maximum cluster separation. By this way, we processed the row measured absorption spectra of differentiating stem cells, and their first and second derivative spectra, in the range 1800–800 cm^{-1}. In all the three cases, excellent segregation of the spectral data into separated clusters – each corresponding to a different time of differentiation – was obtained by PCA-LDA. On the contrary, only the second derivative spectra were partially separated into clusters by simple PCA (data not shown). The classification accuracy of the PCA-LDA was of 86.4% for the measured absorption spectra and for the first derivative, while it increases up to 88.6% for the second derivative spectra.

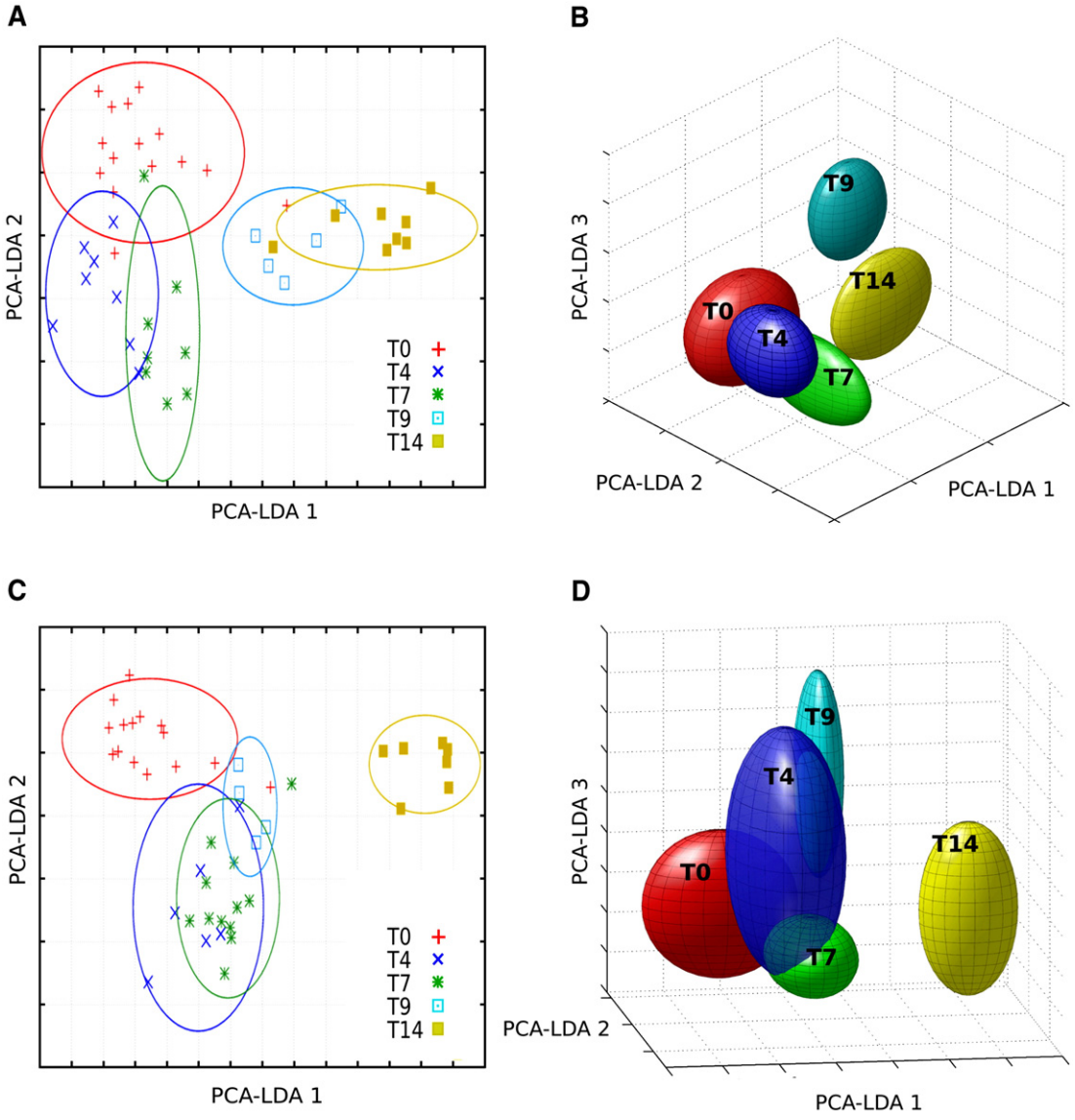

Fig. 5. PCA-LDA score plots of ES cell differentiating FT-IR spectra. Clustering of absorption (A and B) and second derivative (C and D) spectra from 1800 to 800 cm^{-1} are reported as 2D (A and C) and 3D (B and D) score plots. Data for undifferentiated cells and at 4, 7, 9, 14 days of differentiation were analyzed. The semi-axes of ellipses representing each cluster in the 2D plots correspond to two standard deviations of the data; in the 3D plots, the ellipsoid semi-axes are also given by two standard deviations of the data.

In Fig. 5 the PCA-LDA score plots of the most significant discriminant functions are presented for the measured spectra and for their second derivatives. The two-dimensional (2D) score plots are reported in Fig. 5A and C, respectively, for the stem cell row absorption spectra and for their second derivatives at time 0 (undifferentiated cells), 4, 7, 9, 14 days of differentiation. Undifferentiated and 14-day differentiated cells are clearly separated by the first two PCA-LDA scores, while clusters of cell spectra at intermediate differentiation times are partially overlapped. When the third PCA-LDA score is also taken into account, an excellent separation of the five clusters is obtained (Fig. 5B and D). For instance, clusters of row spectra at time 9 and 14 days – overlapped in the 2D plot – become well separated in the 3D plot (Fig. 5A and B). Similarly, for the second derivative spectra, clusters at time 7 and 9 days are separated in the 3D plot (Fig. 5C and D).

Interestingly, PCA-LDA allows also to identify which wavenumbers in the complex FT-IR spectra are responsible for the largest inter-spectral variance [14] that in our case might indicate possible marker bands of differentiation. This can be done through the evaluation of the extent (loading) to which the different wavenumbers contribute to each discriminant functions. By this procedure, we identified the wavenumbers with higher PCA-LDA loadings (see Material and methods) for the stem cell row absorption spectra, and their first and second derivatives. Since the highest variance was found in the 1800–1600 cm^{-1} and in the 1050–800 cm^{-1} regions, the second derivative spectra were processed by PCA-LDA also in these reduced ranges. Again in both cases, an excellent clustering into five well-separated groups was obtained (data not shown). The wavenumbers with higher loadings from this PCA-LDA are reported in Table 1 and compared with the peak positions taken

directly from the second derivative spectra. The highest loadings were found at 1656.1 cm^{-1}, 1658.0 cm^{-1} and at 958.7 cm^{-1}, 954.9 cm^{-1}, 962.6 cm^{-1}, corresponding to the peak positions observed in the second derivative spectra at 1656.7 cm^{-1}, at 954.5 cm^{-1}, and at 966.0 cm^{-1} (Fig. 3 and Table 1). Considering also the time dependence of these FT-IR bands during differentiation (see previous paragraphs), the PCA-LDA results identify these bands as marker bands of differentiation.

4. Discussion

The recent isolation of pluripotent human ES cells from the inner cell mass of blastocyst-stage embryos has raised great hopes for the potential use of these cells in therapeutic transplantation and regenerative medicine, due to the capacity of ES cells to differentiate into different phenotypes, such as cardiomyocytes, neurons, and osteoblasts [32]. To identify and characterize ES cell differentiation, a number of molecular biology techniques are available. Among them, RT-PCR and microarrays technologies, RNA *in situ* hybridisation and immunocytochemistry allow to monitor the expression of specific genes. Even if these approaches enable to obtain detailed information on single differentiation events, non-invasive and rapid methods to characterize ES cells differentiation would be of great relevance and impact in biomedicine.

With this aim, we explored the potential of FT-IR spectroscopy to monitor the spontaneous differentiation process of ES cells. Indeed, among spectroscopic techniques, FT-IR and Raman microspectroscopies [10] have been proved to be powerful tools to investigate at molecular level complex biological systems, with several diagnostic applications in biomedicine [7–11,14–16,45]. In particular, important results on stem cell characterization and differentiation were recently obtained by FT-IR microspectroscopy implemented with multivariate analysis [17–19].

Here, we report a FT-IR microspectroscopy study to monitor simultaneously changes in the response of nucleic acids and proteins expressed by murine ES cells during spontaneous differentiation. By this technique, we obtained in a few minutes an infrared absorption spectrum from a limited number of ES cells, taken directly from their culture. The use of PCA-LDA [13,14] enabled us to explore efficiently the spectra, in spite of their complexity. In particular, a separation of the spectra into clusters corresponding to different times of differentiation was obtained, identifying the infrared bands that bring the largest inter-spectral variance. In this way, marker bands of differentiation were found in the absorption region of nucleic acids and proteins, allowing to monitor the different steps of differentiation within the first 14 days of ES cell culture.

Important insights on the newly acquired phenotype were obtained by the temporal evolution of the ES cell spectra in the region of the amide I band (1700–1600 cm^{-1}), showing that, 4 days after beginning of differentiation, proteins rich in α-helix and β-turn secondary structures started to be expressed by the cells. Interestingly, alpha myosin and connexin, which are specific proteins expressed by ES cells differentiating into cardiomyocyte precursors, both contain these secondary structure elements. As confirmed by PAS reaction, cardiomyocyte precursors were the main new phenotype into which our ES cells differentiated.

Furthermore, in the absorption spectra collected between days 4 and 7 of differentiation, an intensity decrease was observed for two bands in the nucleic acid absorption region, at 994 cm^{-1} and at 914 cm^{-1}, both assigned to ribose vibrations. The simultaneous occurrence of these RNA changes with those observed in the protein amide I band suggested that, in the span of time from day 4 to 7, mRNA translation took place. It is likely that the ES cell reservoir of dormant mRNA could be polyadenylated and activated to produce the proteins that specifically mark the acquisition of the new phenotype. These conclusions are supported by similar results on murine ES cell differentiation recently reported in literature [23,24]. By Raman microspectroscopy, these authors observed – in the early stages of differentiation – a decrease of the Raman RNA band intensity at 813 cm^{-1}, possibly due to the involvement of the cell RNA in the production of the specific proteins for the new phenotype.

Our FT-IR study highlights, in addition, that between days 4 and 7 of differentiation the active transcription of the genome was switched on, as indicated by the appearance of new bands at 954 cm^{-1} and at 899 cm^{-1}. Indeed, the simultaneous presence of these bands, that can be respectively assigned to the C–C vibration of the A-DNA backbone and to the deoxyrybose ring vibration [44], proved that a DNA/RNA hybrid was formed, suggesting that the de novo gene transcription started at this stage of differentiation.

The FT-IR and PCA-LDA approaches presented here allowed, therefore, to identify marker bands of ES cell differentiation. By their time dependence, it has been possible to detect at molecular level, simultaneously, the biological events of ES cell differentiation as they take place, and to monitor in a rapid way the temporal evolution of the ES cell culture.

Acknowledgements

We are grateful to Astrid Gräslund (Stockholm University) for reading the manuscript and to Luca De Gioia (University of Milano-Bicocca) for the helpful discussions on multivariate analysis. We acknowledge the financial support of INFM 2004 and the F.A.R. (Fondo d'Ateneo per la Ricerca) grants to S.M.D.; COFIN MIUR, F.A.R. and Fondazione Cariplo grants to C.A.R.

References

[1] M.J. Evans, M.H. Kaufman, Establishment in culture of pluripotential cells from mouse embryos, Nature 292 (1981) 154–156.
[2] J.A. Thomson, J. Itskovitz-Eldor, S.S. Shapiro, M.A. Waknitz, J.J. Swiergiel, V.S. Marshall, J.M. Jones, Embryonic stem cell lines derived from human blastocysts, Science 282 (1998) 1145–1147.
[3] A.G. Smith, Embryo-derived stem cells: of mice and men, Annu. Rev. Cell Dev. Biol. 17 (2001) 435–462.
[4] P.H. Lerou, G.Q. Daley, Therapeutic potential of embryonic stem cells, Blood Rev. 19 (2005) 321–331.

[5] T. Doetschman, H. Eistetter, M. Katz, W. Schmidt, R. Kemler, The *in vitro* development of blastocyst-derived embryonic stem cell lines: formation of visceral yolk sac, blood islands and myocardium, J. Embryol. Exp. Morphol. 87 (1985) 27–45.
[6] G. Weitzer, Embryonic stem cell-derived embryoid bodies: an *in vitro* model of eutherian pregastrulation development and early gastrulation, Handb. Exp. Pharmacol. 174 (2006) 21–51.
[7] D. Naumann, D. Helm, H. Labischinski, Microbiological characterizations by FT-IR spectroscopy, Nature 351 (1991) 81–82.
[8] B.R. Wood, B. Tait, D. McNaughton, Fourier transform infrared spectroscopy as a method for monitoring the molecular dynamics of lymphocyte activation, Appl. Spectrosc. 54 (2000) 353–359.
[9] L.P. Choo-Smith, K. Maquelin, T. Van Vreeswijk, H.A. Bruining, G.J. Puppels, N.A. Ngo Thi, C. Kirschner, D. Naumann, D. Ami, A.M. Villa, F. Orsini, S.M. Doglia, H. Lamfarraj, G.D. Sockalingum, M. Manfait, P. Allouch, H.P. Endtz, Investigating microbial (micro)colony heterogeneity by vibrational spectroscopy, Appl. Environ. Microbiol. 67 (2001) 1461–1469.
[10] D. Naumann, FT-infrared and FT-Raman spectroscopy in biomedical research, in: H.-U. Gremlich, B. Yan (Eds.), Infrared and Raman Spectroscopy of Biological Materials. Practical Spectroscopy, Marcel Dekker, New York, USA, 2000.
[11] A. Kretlow, Q. Wang, J. Kneipp, P. Lasch, M. Beekes, L. Miller, D. Naumann, FTIR-microspectroscopy of prion-infected nervous tissue, Biochim. Biophys. Acta 1758 (2006) 948–959.
[12] E.P. Pourmand, I. Binderman, S.B. Doty, V. Kudryashov, A.L. Boskey, Chondrocyte apoptosis is not essential for cartilage calcification: evidence from an *in vitro* avian model, J. Cell. Biochem. 100 (2007) 43–57.
[13] T. Fearn, Discriminant analysis, in: J.M. Chalmers, P.R. Griffiths (Eds.), Handbook of Vibrational Spectroscopy, vol. 3, Wiley, New York, 2002, pp. 2086–2093.
[14] M.J. Walsh, M.N. Singh, H.M. Pollock, L.J. Cooper, M.J. German, H.F. Stringfellow, N.J. Fullwood, E. Paraskevaidis, P.L. Martin-Hirsch, F.L. Martin, ATR microspectroscopy with multivariate analysis segregates grades of exfoliative cervical cytology, Biochem. Biophys. Res. Commun. 352 (2007) 213–219.
[15] M.J. German, A. Hammiche, N. Ragavan, M.J. Tobin, L.J. Cooper, S.S. Matanhelia, A.C. Hindley, C.M. Nicholson, N.J. Fullwood, H.M. Pollock, F.L. Martin, Infrared spectroscopy with multivariate analysis potentially facilitates the segregation of different types of prostate cell, Biophys. J. 90 (2006) 3783–3795.
[16] A. Hammiche, M.J. German, R. Hewitt, H.M. Pollock, F.L. Martin, Monitoring cell cycle distributions in MCF-7 cells using near-field photothermal microspectroscopy, Biophys. J. 88 (2005) 3699–3706.
[17] M.J. German, H.M. Pollock, B. Zhao, M.J. Tobin, A. Hammiche, A. Bentley, L.J. Cooper, F.L. Martin, N.J. Fullwood, Characterization of putative stem cell populations in the cornea using synchrotron infrared microspectroscopy, Invest. Ophthalmol. Vis. Sci. 47 (2006) 2417–2421.
[18] A.J. Bentley, T. Nakamura, A. Hammiche, H.M. Pollock, F.L. Martin, S. Kinoshita, N.J. Fullwood, Characterization of human corneal stem cells by synchrotron infrared micro-spectroscopy, Mol. Vis. 13 (2007) 237–242.
[19] C. Krafft, R. Salzer, S. Seitz, C. Ern, M. Schieker, Differentiation of individual human mesenchymal stem cells probed by FTIR microscopic imaging, Analyst 132 (2007) 647–653.
[20] B.J. Willenberg, T. Hamazaki, F.-W. Meng, N. Terada, C. Batich, Self-assembled copper-capillary alginate gel scaffolds with oligochitosan support embryonic stem cell growth, J. Biomed. Mater. Res. A 79 (2006) 440–450.
[21] T. Nakaji-Hirabayashi, K. Kato, Y. Arima, H. Iwata, Oriented immobilization of epidermal growth factor onto culture substrates for the selective expansion of neural stem cells, Biomaterials 28 (2007) 3517–3529.
[22] D. Horak, M. Babic, P. Jendelova, V. Herynek, M. Trchova, Z. Pientka, E. Pollert, M. Hajek, E. Sykova, D-Mannose-modified iron oxide nanoparticles for stem cell labelling, Bioconjug. Chem. 18 (2007) 635–644.
[23] L. Notingher, I. Bisson, J.M. Polak, L.L. Hench, *In situ* spectroscopic study of nucleic acids in differentiating embryonic stem cells, Vib. Spectrosc. 35 (2004) 199–203.
[24] I. Notingher, I. Bisson, A.E. Bishop, W.L. Randle, J.M.P. Polak, L.L. Hench, *In situ* spectral monitoring of mRNA translation in embryonic stem cells during differentiation *in vitro*, Anal. Chem. 76 (2004) 3185–3193.
[25] J.L.R. Arrondo, F.M. Goni, Structure and dynamics of membrane proteins as studied by infrared spectroscopy, Prog. Biophys. Mol. Biol. 72 (1999) 367–405.
[26] A. Barth, C. Zscherp, What vibrations tell us about proteins, Q. Rev. Biophys. 35 (2002) 369–430.
[27] D. Ami, L. Bonecchi, S. Calì, G. Orsini, G. Tonon, S.M. Doglia, FT-IR study of heterologous protein expression in recombinant *Escherichia coli* strains, Biochim. Biophys. Acta 1624 (2003) 6–10.
[28] D. Ami, A. Natalello, P. Gatti-Lafranconi, M. Lotti, S.M. Doglia, Kinetics of inclusion body formation studied in intact cells by FT-IR spectroscopy, FEBS Lett. 579 (2005) 3433–3436.
[29] D. Ami, A. Natalello, G. Taylor, G. Tonon, S. Maria Doglia, Structural analysis of protein inclusion bodies by Fourier transform infrared microspectroscopy, Biochim. Biophys. Acta 1764 (2006) 793–799.
[30] L.P. Choo, D.L. Wetzel, W.C. Halliday, M. Jackson, S.M. LeVine, H.H. Mantsch, *In situ* characterization of beta-amyloid in Alzheimer's diseased tissue by synchrotron Fourier transform infrared microspectroscopy, Biophys. J. 71 (1996) 1672–1679.
[31] D. Ami, A. Natalello, A. Zullini, S.M. Doglia, Fourier transform infrared microspectroscopy as a new tool for nematode studies, FEBS Lett. 576 (2004) 297–300.
[32] A.M. Wobus, K. Guan, H.T. Yang, K.R. Boheler, Embryonic stem cells as a model to study cardiac, skeletal muscle, and vascular smooth muscle cell differentiation, Methods Mol. Biol. 185 (2002) 127–156.
[33] G. Bain, D. Kitchens, M. Yao, J.E. Huettner, D.I. Gottlieb, Embryonic stem-cells express neuronal properties *in-vitro*, Dev. Biol. 168 (1995) 342–357.
[34] J. Karbanova, J. Mokry, Histological and histochemical analysis of embryoid bodies, Acta Histochem. 104 (2002) 361–365.
[35] K.B.S. Pasumarthi, L.J. Field, Cardiomyocyte enrichment in differentiating ES cell cultures: strategies and applications, in: K. Turksen (Ed.), Embryonic Stem Cells Methods and Protocols, Humana Press, New Jersey, 2002, pp. 157–168.
[36] F. Orsini, D. Ami, A.M. Villa, G. Sala, M.G. Bellotti, S.M. Doglia, FT-IR microspectroscopy for microbiological studies, J. Microbiol. Methods 42 (2000) 17–27.
[37] W.W. Colley, P.R. Lohnes, Multivariate Data Analysis, Wiley, 1971.
[38] A. Nagy, M. Gertsenstein, K. Vintersten, R. Behringer, Manipulating the Mouse Embryo, a Laboratory Manual, Cold Spring Harbor Laboratory, New York, 2003.
[39] T. Neri, M. Monti, P. Rebuzzini, V. Merico, S. Garagna, C.A. Redi, M. Zuccotti, Mouse fibroblasts are reprogrammed to *Oct-4* and *Rex-1* gene expression and alkaline phosphatase activity by embryonic stem cell extracts, Cloning Stem Cells 9 (2007) 394–406.
[40] J. Heo, J.S. Lee, I.S. Chu, Y. Takahama, S.S. Thorgeirsson, Spontaneous differentiation of mouse embryonic stem cells *in vitro*: characterization by global gene expression profiles, Biochem. Biophys. Res. Commun. 332 (2005) 1061–1069.
[41] A. Dong, P. Huang, W.S. Caughey, Protein secondary structures in water from 2nd-derivative amide-i infrared-spectra, Biochemistry 29 (1990) 3303–3308.
[42] Y. Oyamada, K. Komatsu, H. Kimura, M. Mori, M. Oyamada, Differential regulation of gap junction protein (connexin) genes during cardiomyocytic differentiation of mouse embryonic stem cells *in vitro*, Exp. Cell Res. 229 (1996) 318–326.
[43] J. Liquier, E. Taillandier, Infrared spectroscopy of nucleic acids, in: H.H. Mantsch, D. Chapman (Eds.), Infrared Spectroscopy of Biomolecules, Wiley-Liss, Inc, New York, 1996, pp. 131–158.
[44] M. Banyay, M. Sarkar, A. Graslund, A library of IR bands of nucleic acids in solution, Biophys. Chemist. 104 (2003) 477–488.
[45] C. Kirschner, K. Maquelin, P. Pina, N.A.N. Thi, L.P. Choo-Smith, G.D. Sockalingum, C. Sandt, D. Ami, F. Orsini, S.M. Doglia, P. Allouch, M. Mainfait, G.J. Puppels, D. Naumann, Classification and identification of enterococci: a comparative phenotypic, genotypic, and vibrational spectroscopic study, J. Clin. Microbiol. 39 (2001) 1763–1770.